# Supporting Information

# $FeF_3 \cdot 0.33H_2O$@Carbon Nanosheets with Honeycomb Architectures for High-capacity Lithium-ion Cathode Storage by Enhanced Pseudocapacitance

Liguo Zhang,[a] Litao Yu,[a] Oi Lun Li,*[a] Si Young Choi,[c] Ghuzanfar Saeed,[b] and Kwang Ho Kim,*[ab]

[a]Department of Materials Science and Engineering, Pusan national University, 2 Busandaehak-ro 63 beon-gil, Geumjeong-gu, Busan 46241, Republic of Korea

[b]Global Frontier R&D Center for Hybrid Interface Materials, Pusan national University, 2 Busandaehak-ro 63 beon-gil, Geumjeong-gu, Busan 46241, Republic of Korea

[c]Department of Materials Science and Engineering, Pohang University of Science and Technology, 77 Cheongam-Ro, Nam-Gu, Pohang, Gyeongbuk 37673, Republic of Korea

*E-mail: helenali@pusan.ac.kr

*E-mail: kwhokim@pusan.ac.kr

## Experimental Details

### Synthesis of the bare $FeF_3 \cdot 0.33H_2O$

The $FeF_3 \cdot 0.33H_2O$ was synthesized using hydrogen fluoride (HF) as a fluorine source, and iron (III) nitrate nonahydrate ($Fe(NO_3)_3 \cdot 9H_2O$) as an iron source. In the typical synthesis of composite materials by hydrothermal reaction, 1.0 mL HF was added to a 100 mL Teflon beaker containing 50 mL isopropanol. Under magnetic stirring, add 2.02 g $Fe(NO_3)_3 \cdot 9H_2O$ to the above solution to dissolve it. After stirring for 20 minutes, the above solution in the Teflon autoclave was put in an oven and was heated for 12 hours at 150 °C. It was then cooled at room temperature to obtain an off-white precipitate. The precipitate was washed with ethanol and dried under vacuum at 80 °C for 12 hours. After naturally cooling to room temperature, the bare $FeF_3 \cdot 0.33H_2O$ was gained.

### Synthesis of CNS Carbon (Carbon Nanosheets Carbon)

For obtaining CNS Carbon (Carbon Nanosheets Carbon), the $Fe_3C$@CNS was immersed in HCl (10%) solution for 5h. After ultrasonic treatment, The precipitated particles were washed with centrifugation, and dried in the oven.

### Synthesis of LCNS (Pre-lithiated Carbon Nanosheets)

Pre-lithiation process of **CNS** electrode was carried out by galvanostatic discharging in coin cell (CR2416) which assembled with CNS working electrode and lithium countering electrode. The pre-lithiation process was terminated once the capacity of the cell reached 0.01V.

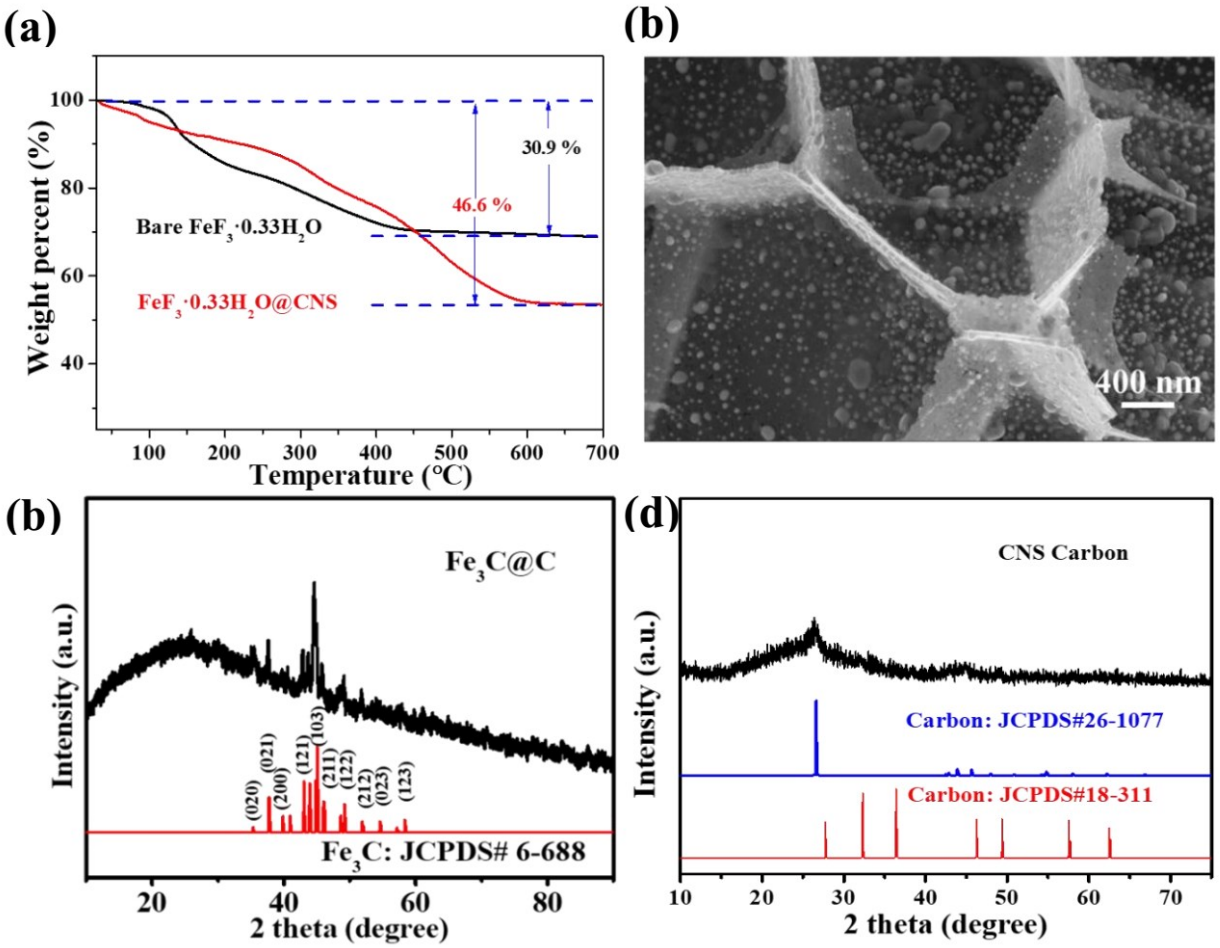


**Fig. S1.** (a) Thermogravimetric analysis (TGA) of $FeF_3 \cdot 0.33H_2O$@CNS and bare $FeF_3 \cdot 0.33H_2O$; (b) SEM images of uniform $Fe_3C$@C nanosheets; (c) XRD pattern of $Fe_3C$@C nanosheets being consistent with $Fe_3C$; (d) XRD pattern of the CNS Carbon obtained by etching $Fe_3C$@CNS with HCl solution, being consistent with Carbon.

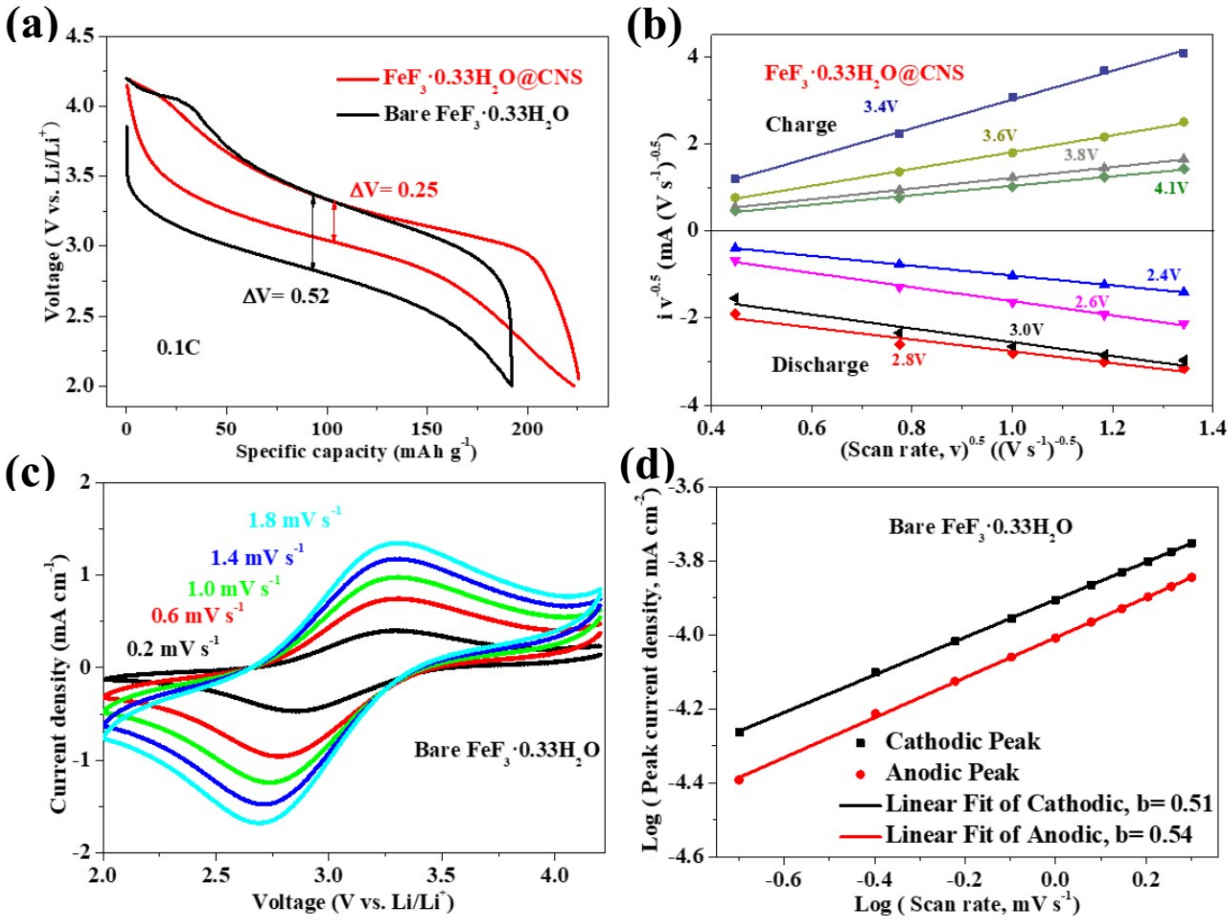


**Fig. S2.** (a) Galvanostatic charging/ discharging curves comparative of the $FeF_3{\cdot}0.33H_2O$@CNS electrode and the bare $FeF_3{\cdot}0.33H_2O$ electrode; (b) Relationship between current /(scan rate)$^{1/2}$ and (scan rate)$^{1/2}$of $FeF_3{\cdot}0.33H_2O$@CNS electrode for calculating constants $k_1$ and $_{k2}$ at different potentials; (c) CV curves at di□erent scan rates of the bare $FeF_3{\cdot}0.33H_2O$ electrode; (d) Relationship between Log (current density) and Log(scan rate) of the bare $FeF_3{\cdot}0.33H_2O$ electrode for calculating b value.

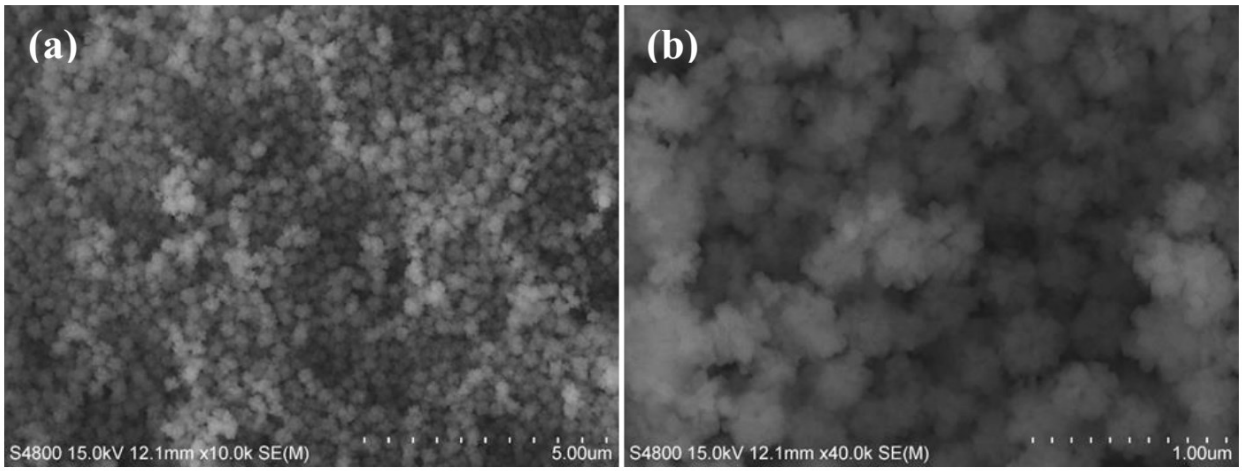


**Fig. S3.** SEM characterizations of the bare $FeF_3 \cdot 0.33H_2O$

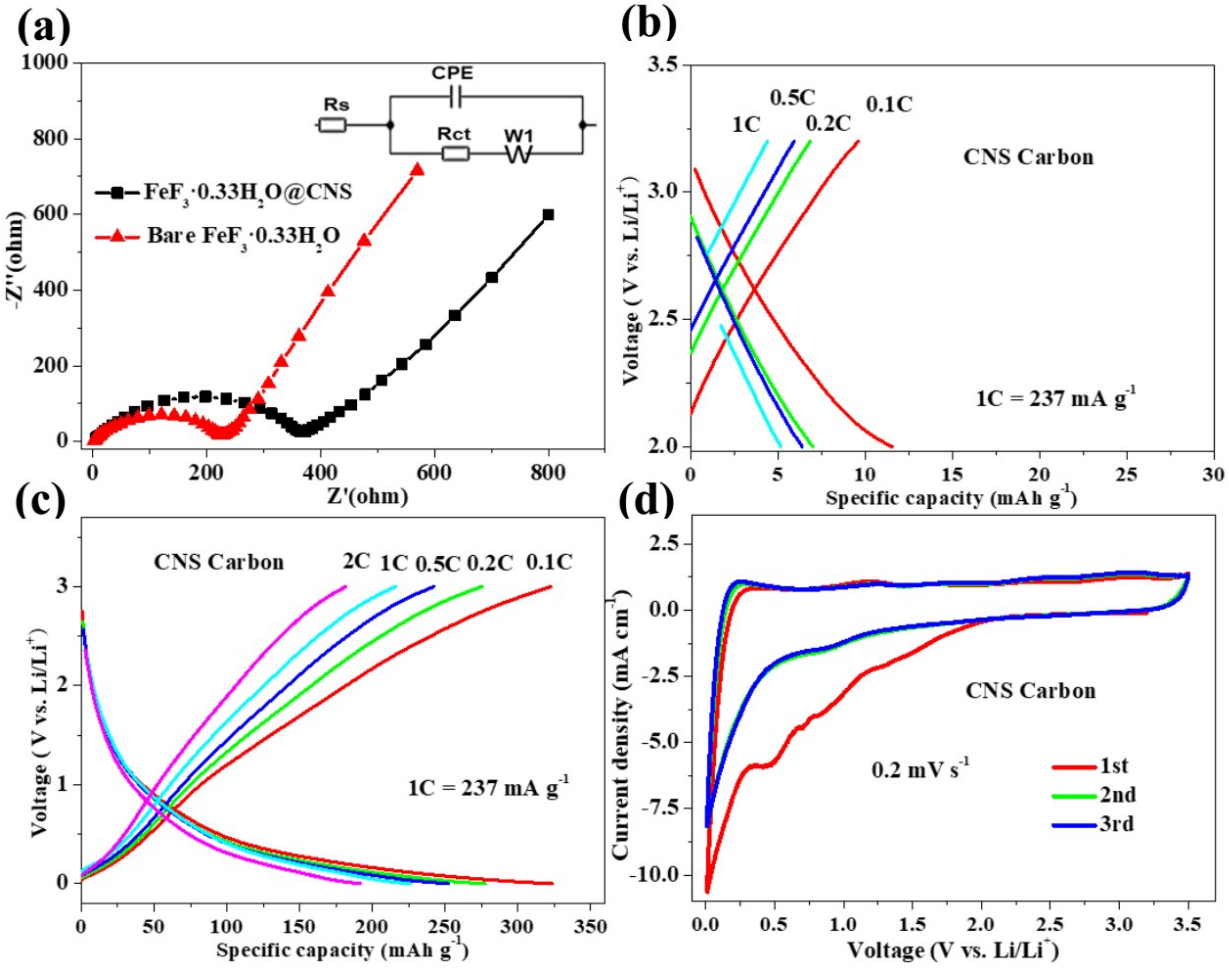


**Fig. S4**. (a) Nyquist plots measured for the $FeF_3 \cdot 0.33H_2O$@CNS electrode and bare $FeF_3 \cdot 0.33H_2O$ electrode (Inset: the simplified equivalent circuit model); (b) The rate performance curves of the CNS Carbon cathode with a voltage range of 2.0- 3.2 V (vs. $Li/Li^+$), which show that the cathode capacity of pure carbon CNS under high cathode voltage is almost negligible. The electrode of the CNS Carbon cathode can be damaged when charged at a voltage higher than 3.2V; (c) The rate performance curves of the CNS Carbon anode with a voltage range of 0.01- 3.0 V (vs. $Li/Li^+$); (d) Cyclic voltammograms of the CNS Carbon electrode scanned with a voltage range of 0.01–3.5 V (vs. $Li/Li^+$) at a scan rate of 0.2 mV $s^{-1}$.

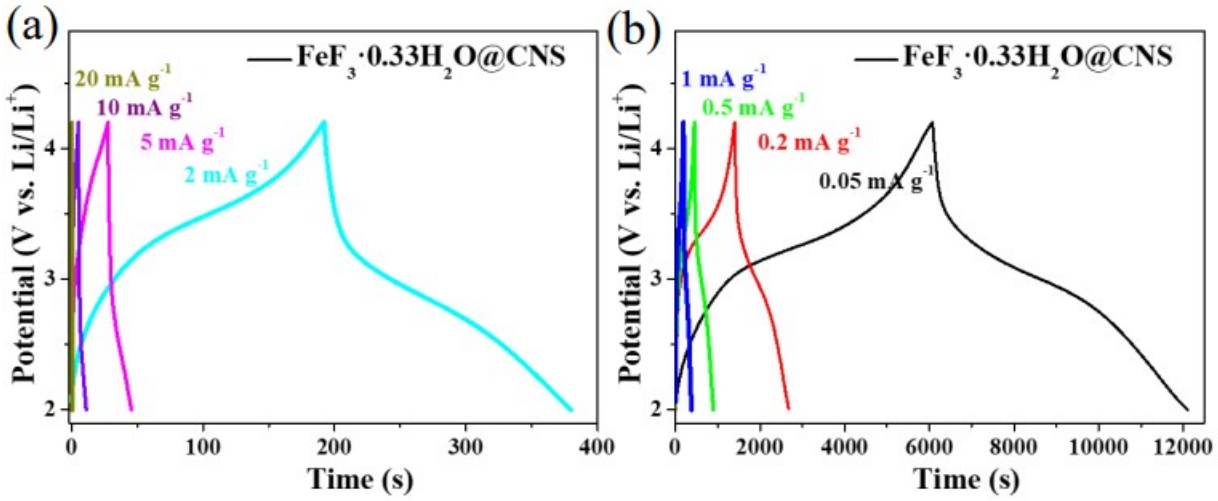


**Fig. S5**. Li-ion supercapacitance characterization of the $FeF_3 \cdot 0.33H_2O$@CNS//Li: The galvanostatic charging/ discharging profiles from 2 to 4.2V at high current densities (a) and low current densities (b). the results shows that the $FeF_3 \cdot 0.33H_2O$@CNS exhibit excellent electrochemical performance at low current densities, but exhibit bad performance at low current densities. supercapacitors are used for high current and high power, therefore the $FeF_3 \cdot 0.33H_2O$@CNS is not suitable for supercapacitors.

**Table S1.** The comparison of discharge capacities and fading rates/ cycle of the previously reported $FeF_3$ electrodes.

| Electrode | Voltage range (V) | Current density (mA $g^{-1}$) | Discharge capacity (mAh $g^{-1}$) /(cycle no.) | Ref. |
|---|---|---|---|---|
| **$FeF_3 \cdot 0.33H_2O$/ Graphene & CNTs** | **1.5- 4.5** | **162 (1C)** | **200/($2^{nd}$)-146/($100^{th}$)** | [1] |
| **$FeF_3 \cdot 0.33H_2O$/ 3D rGO** | **2.0- 4.5** | **200 (1C)** | **202/($1^{st}$)- 167/($50^{th}$)** | [2] |
| **$FeF_3 \cdot 0.33H_2O$** | **2.0- 4.5** | **200 (1C)** | **145/($1^{st}$)- 130/($200^{th}$)** | [3] |
| **$FeF_3 \cdot 0.33H_2O$/ N-doped 3D Porous Carbon** | **2.0- 4.5** | **200 (1C)** | **163/($1^{st}$)- 146.7/($200^{th}$)** | [4] |
| **$FeF_3 \cdot 0.33H_2O$/ rGO** | **1.7- 4.5** | **100 (0.5C)** | **175/($1^{st}$)- 171.5/($100^{th}$)** | [5] |
| **$FeF_3 \cdot 0.33H_2O$/ Graphene & CNTs** | **1.8- 4.5** | **45 (0.2C)** | **225/($1^{st}$)- 222.8/($50^{th}$)** | [6] |
| **Hollow Spheres $FeF_3 \cdot 0.33H_2O$** | **1.5- 4.2** | **712 (3C)** | **169/($1^{st}$)- 163.4/($40^{th}$)** | [7] |
| **$FeF_3 \cdot 0.33H_2O$ with active site exposed** | **2.0-4.5** | **200 (1C)** | **163/($1^{st}$)- 146.7/($30^{th}$)** | [8] |
| **$FeF_3 \cdot 0.33H_2O$@C** | **2.0- 4.5** | **200 (1C)** | **178/($2^{nd}$)- 172.9/($200^{th}$)** | **This work** |

**References**

[1] Q. Zhang, Y. Zhang, Y. Yin, L. Fan, N. Zhang, J. Power Sources, 447 (2020) 227303.
[2] S. Chen, J. Lin, Q. Shi, Z. Cai, L. Cao, L. Zhu, Z. Yuan, J. Electrochem. Soc., 167 (2020) 080506.
[3] H. Zhou, H. Sun, T. Wang, Y. Gao, J. Ding, Z. Xu, J. Tang, M. Jia, J. Yang, J. Zhu, Inorg. Chem., 58 (2019) 6765-6771.
[4] Q. Zhang, X. Wu, S. Gong, L. Fan, N. Zhang, ChemistrySelect, 4 (2019) 10334-10339.
[5] J. Zhai, Z. Lei, D. Rooney, K. Sun, Electrochimica Acta, 313 (2019) 497-504.
[6] L. Lu, S. Li, J. Li, L. Lan, Y. Lu, S. Xu, S. Huang, C. Pan, F. Zhao, Nanoscale Res. Lett., 14 (2019) 100.
[7] J. Lin, L. Zhu, S. Chen, Q. Li, Z. He, Z. Cai, L. Cao, Z. Yuan, J. Liu, J. Electrochem. Soc., 166 (2019) A2074-A2082.
[8] G. Chen, X. Zhou, Y. Bai, Y. Yuan, Y. Li, M. Chen, L. Ma, G. Tan, J. Hu, Z. Wang, F. Wu, C. Wu, J. Lu, Nano Energy, 56 (2019) 884-892.